Cancer Chemother Pharmacol (1998) 41: 201–209

ORIGINAL ARTICLE

Lillian L. Habeck · Sylvia H. Chay
Raymond C. Pohland · John F. Worzalla
Chuan Shih · Laurane G. Mendelsohn

Whole-body disposition and polyglutamate distribution of the GAR formyltransferase inhibitors LY309887 and lometrexol in mice: effect of low-folate diet

Received: 19 November 1996 / Accepted: 12 May 1997

Abstract *Purpose*: The whole-body autoradiographic distribution of two radiolabeled antifolate inhibitors of GAR formyltransferase, lometrexol and LY309887, were compared in tumor-bearing mice maintained on standard diet (SD) and a low-folate diet (LFD) in order to determine the total amounts of drug that accumulated in blood, tumor, liver and kidney. The time-dependent changes in tissue distribution were evaluated over a 7-day period in order to compare the pharmacokinetic properties of both inhibitors and to assess the influence of dietary folate on this distribution. In addition, the effect of dietary folate on polyglutamation of compound accumulating in the liver was measured. The results have bearing on the potential of these two clinical agents to produce delayed toxicity in cancer patients and the use of dietary folate to modulate or prevent the development of this toxicity. *Methods*: Single equimolar i.v. doses of [^{14}C]LY309887 and [^{14}C]lometrexol were administered to C3H mammary tumor bearing mice on SD or LFD, and the disposition of these compounds was quantitated using whole-body autoradiography. Livers were also harvested and extracted for determination of polyglutamate distribution. Animals were sacrificed both early and late (7 days) after dosing to determine the long-term retention of these compounds. *Results*: Whole-body autoradiography revealed that the highest concentrations of both compounds were in liver and kidney. Concentrations of both compounds were two-fold higher in livers from LFD mice than in livers from SD mice. Lometrexol concentrations in liver averaged 2.8- and 2.2-fold higher than LY309887 in SD and LFD livers, respectively. In SD livers, the polyglutamate profiles of both compounds were similar, with hexaglutamates being the longest chain species detected. In LFD livers, hexaglutamates of LY309887 were observed, while hepta- and octaglutamates of lometrexol were detected after 168 h. *Conclusions*: The reduced hepatic retention and biochemical profile of LY309887 compared to lometrexol suggest that it may be less likely to produce delayed cumulative toxicity while still retaining antitumor activity. However, the increased hepatic accumulation observed in LFD mice emphasizes the importance of assessing and supplementing folate in cancer patients treated with this class of compounds.

Key words GARFT · Polyglutamation · Delayed toxicity · Hepatic retention

L.L Habeck · J.F. Worzalla · C. Shih · L.G. Mendelsohn (✉)
Department of Cancer Research, Lilly Research Laboratories, Indianapolis, Indiana 46285, USA

S.H. Chay · R.C. Pohland
Toxicology Research Laboratories, Lilly Research Laboratories, Greenfield, Indiana 46140, USA

Introduction

LY309887 is a novel inhibitor of glycinamide ribonucleotide formyltransferase (GARFT) [8], the first folate-dependent enzyme of purine *de novo* synthesis, and is currently in phase 1 clinical trials for treatment of solid tumors. LY309887 differs from lometrexol [(6*R*)-5,10-dideazatetrahydrofolate], the first selective inhibitor of GARFT [14], by replacement of the phenyl moiety with a 2′,5′-thienyl group (Fig. 1). This modification enhances its potency in inhibiting human GARFT ninefold, as the K_i values are 6.5 and 59.7 n*M*, respectively [8]. Like lometrexol, LY309887 possesses a broad spectrum of activity against a panel of solid murine and human xenograft tumors [8, 12] and is a substrate for folylpolyglutamate synthetase (FPGS) [9], which catalyzes the addition of glutamic acid residues. Polyglutamation of antifolates has been shown to increase affinity for certain folate-dependent enzymes [2, 8, 23], as well as increase cellular retention [11]. LY309887 binds to the folate receptor [8], one of the routes by which folates and antifolates are transported into cells. Different isoforms of the folate receptor, with different affinities for antifolates, are expressed in murine and human tumors, liver, and kidney [3, 6, 18, 22].

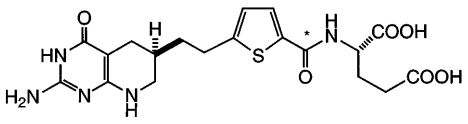

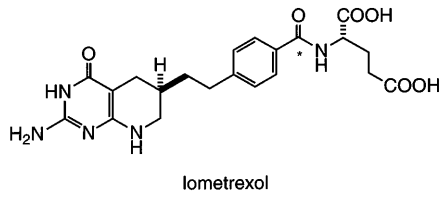

Fig. 1 Chemical structures of LY309887 and lometrexol. LY309887 is an analogue of lometrexol in which the phenyl ring has been replaced by a 2′,5′-thienyl group. The * denotes location of radiolabel on LY309887 and lometrexol (6*R*-5,10-dideazatetrahydrofolate)

In preclinical tumor models, LY309887 has been shown to be more potent than lometrexol [12]. Maximal antitumor activity was observed at 30–40 mg/kg per dose (every 3 days × 4 schedule), while lometrexol inhibited maximally at 100–200 mg/kg per dose and required more frequent dosing (every 2 days × 5) for optimal efficacy.

In phase 1 clinical studies with lometrexol, severe delayed cumulative toxicity has been encountered (thrombocytopenia and anemia) which was not predicted by the preclinical murine studies [16]. Subsequently, a low-folate diet (LFD) murine model revealed greater than 100-fold increased toxicity of lometrexol in mice maintained on LFD than in those on a standard diet (SD). Supplementation with oral folic acid eliminates the increased toxicity in LFD mice and restores antitumor activity [1]. Whole-body autoradiographic studies have shown up to a four-fold greater hepatic retention of lometrexol in LFD mice than in SD mice [15]. Folic acid supplementation reduces liver deposition by 50% and provides complete protection against toxicity. LFD mice also maintain higher plasma levels of lometrexol significantly longer than SD mice. Sustained plasma levels resulting in prolonged exposure of renewable tissues such as bone marrow and gastrointestinal epithelium to drug may contribute to delayed toxicity. Additional studies have demonstrated that changes in dietary folate intake of tumor-bearing mice alter the folate status of murine organs [19]. In phase 1 clinical trials with lometrexol, supplemental folic acid has been shown to eliminate the cumulative toxicity while clinical responses are still observed [27]. It is clear that folate status plays a central role in determining the degree of hepatic retention, plasma half-life, and development of delayed toxicity for lometrexol, by affecting hepatic deposition and clearance. Other mechanisms such as reabsorption following biliary secretion may also modulate lometrexol toxicity.

LY309887 has several properties which suggest that it may have greater antitumor activity and be less likely to produce delayed cumulative toxicity than lometrexol. These properties include: nine-fold greater potency as a GARFT inhibitor [8], inhibition of murine and human xenograft tumor growth at lower doses than lometrexol and a broader spectrum of antitumor activity in xenograft tumors [8, 12], lower affinity for the murine and human liver folate receptor isoforms [6, 12], and a lower efficiency (first-order rate constant, V_{max}/K_m) as a substrate for mammalian FPGS [9]. Collectively, these properties suggest that less activation of LY309887 by polyglutamation would be required to achieve tight-binding inhibition of GARFT and that clinical responses may be achieved at lower doses. Secondly, liver may accumulate and retain less LY309887 because of its lower affinity for liver folate receptors and reduced polyglutamation by liver FPGS. Thus, at equimolar doses, LY309887 may be less likely to accumulate in liver and may be less extensively polyglutamated than lometrexol.

To test this hypothesis, the whole-body autoradiographic disposition of [^{14}C]lometrexol and [^{14}C]-LY309887 was measured over 7 days in tumor-bearing mice maintained on SD or LFD after single intravenous (i.v) equimolar dosing using phosphor imaging technology. The extent of polyglutamation in liver was also determined after harvesting and extraction using reversed-phase HPLC. Equimolar doses were tested to allow a direct comparison of the molar accumulation and metabolism of these two drugs.

Materials and methods

Materials

[^{14}C]Lometrexol (specific activity 7.57 mCi/mmol) and [^{14}C]-LY309887 (specific activity 47.6 and 49.9 mCi/mmol) were synthesized at Lilly Research Laboratories, Indianapolis, Ind. Female C3H mice were obtained from Taconic, Germantown, N.Y. Murine C3H mammary carcinoma was purchased from the Jackson Laboratory (Bar Harbor, Me.) and carried by serial tumor implantation.

Murine diets and dosing regimen

C3H mice were placed on SD (Purina Chow #5001, 5.9 ppm folate) or LFD (Purina Chow #5831C-2, 0.032 ppm folate) for 2 weeks prior to tumor implantation and for the remainder of the study. On day 15, mice were implanted with C3H mammary carcinoma in the left axillary region by trocar [26]. On day 19, mice received a single i.v. bolus dose of [^{14}C]lometrexol (0.72 mg/kg) or an equimolar dose of [^{14}C]LY309887 (0.6 mg/kg) in a vehicle of 0.5 *M* sodium bicarbonate. This dose (1.33 μmol/kg per dose) was the LD_{50} of LY309887 for LFD tumor-bearing mice on an optimal every 3 days × 4 schedule. For comparison, the LD_{10} values (mg/kg per dose) on an every 3 days × 4 schedule were: LY309887 (SD), 30–100; LY309887 (LFD), 0.4; lometrexol (SD), >1000; and lometrexol (LFD), 0.3–1.0. Previous experiments had shown that all mice would survive longer than the 7 days required to complete the study, and all animal experiments were approved by the Lilly Research Laboratories Animal Care and Use Committee. The four

experimental groups were: SD mice treated with [^{14}C]LY309887; LFD mice treated with [^{14}C]LY309887; SD mice treated with [^{14}C]lometrexol; and LFD mice treated with [^{14}C]lometrexol. Each group consisted of 14 mice, 7 for autoradiography and 7 for polyglutamate determination

Quantitative whole-body autoradiographic evaluation

Mice were processed for whole-body autoradiographic evaluation as described in detail by Ullberg [21]. Mice were euthanized with isoflurane, frozen in dry-ice-cooled hexane and stored. The frozen carcasses were embedded with a 2% aqueous carboxymethylcellulose gel (Sigma Chemical Company, St. Louis, Mo.) which when frozen, provided support for sectioning on a cryomicrotome (Leica, Deerfield, il.). Sagittal whole-body sections (approximately 20–40 μm) were freeze-dried, and autoradiographic images were recorded and quantified using phosphor imaging technology as described by Johnston et al. [10]. Whole-body sections were collected to obtain representative samples which included the liver, tumor, blood, and kidney. Radioactivity was quantitated using tissue-calibrated radiocarbon commercial standards (American Radiolabeled Chemicals, St. Louis, Mo.) and liver homogenate containing [^{14}C]glucose at a concentration of 42.8 nCi/g, which was used as an internal standard to correct for section thickness.

Sections and standards were simultaneously exposed for about 7 days for mice receiving [^{14}C]LY309887 and 7 weeks for those receiving [^{14}C]lometrexol to phosphor imaging plates (Molecular Dynamics Sunnyvale, Calif.). Exposure times were adjusted to compensate for the difference in specific activities. Prior to exposure, background was erased by exposing the imaging plates to bright visible light using the Model 410A Image Eraser (Molecular Dynamics). Following exposure, imaging plates were scanned with a helium–neon laser using the Model 425E PhosphorImager (Molecular Dynamics). Scanner operations, data display, and analysis were performed using ImageQuant (Molecular Dynamics) and Excel (Microsoft, Redmond, Wash.) software. Quantitative evaluation was accomplished using volume integrated phosphor imager signals from tissues which were corrected for section thickness variation using the internal standard [4]. Duplicate sampling was performed on multiple sections for each tissue from each animal.

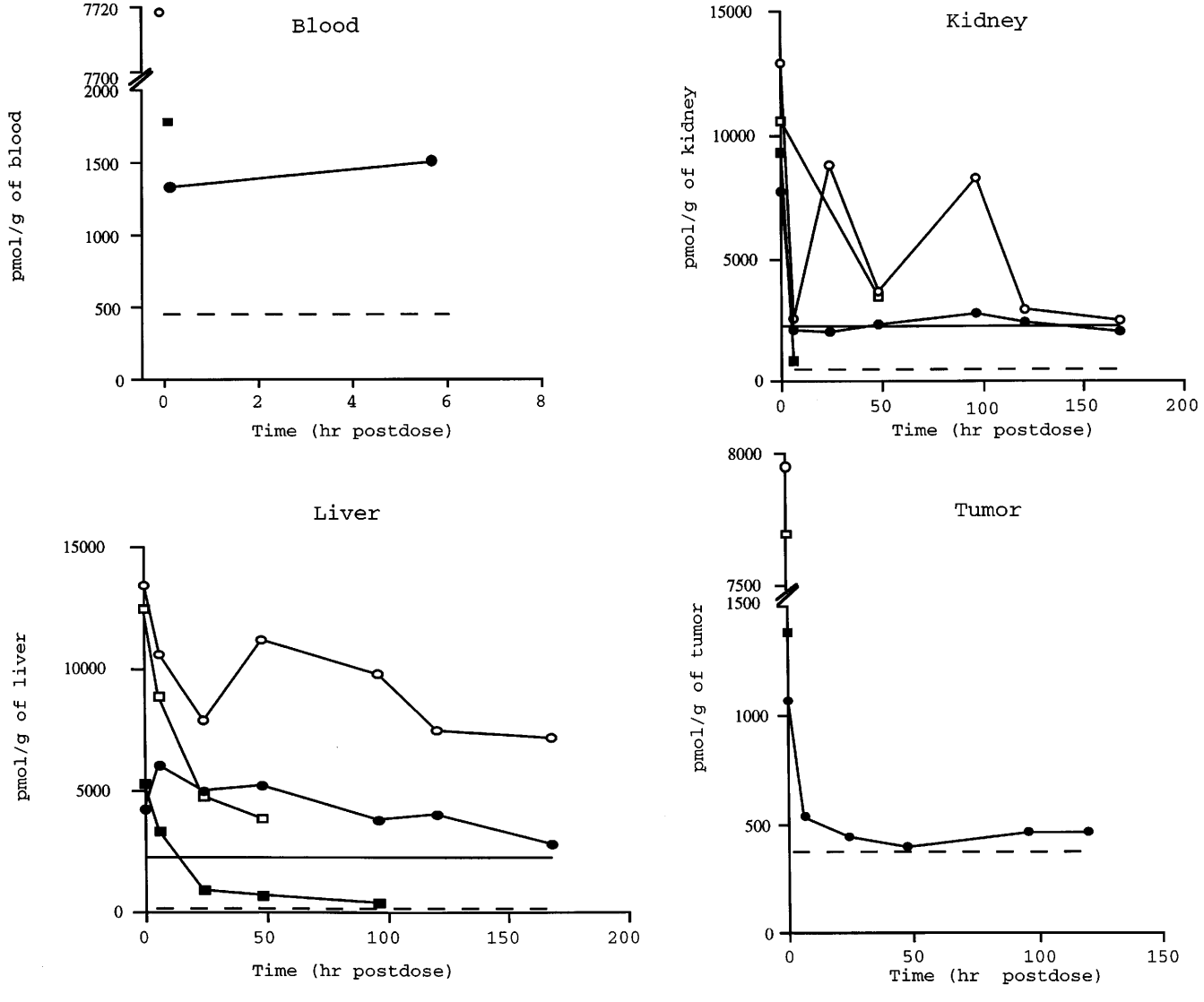

Fig. 2 Tissue disposition of radiocarbon associated with [^{14}C]LY309887 and [^{14}C]lometrexol in blood, kidney, liver, and tumor. After a single equimolor i.v. dose (1.33 μmol/kg), tissue distribution of total radiocarbon was determined by quantitative whole-body autoradiography and is expressed as pmol/g of tissue associated with [^{14}C]LY309887 in mice on LFD (●) and SD (■), and with [^{14}C]lometrexol in mice on LFD (○) and SD (□). The lower limits of detection for [^{14}C]LY309887 (----) and [^{14}C]lometrexol (—) are also shown

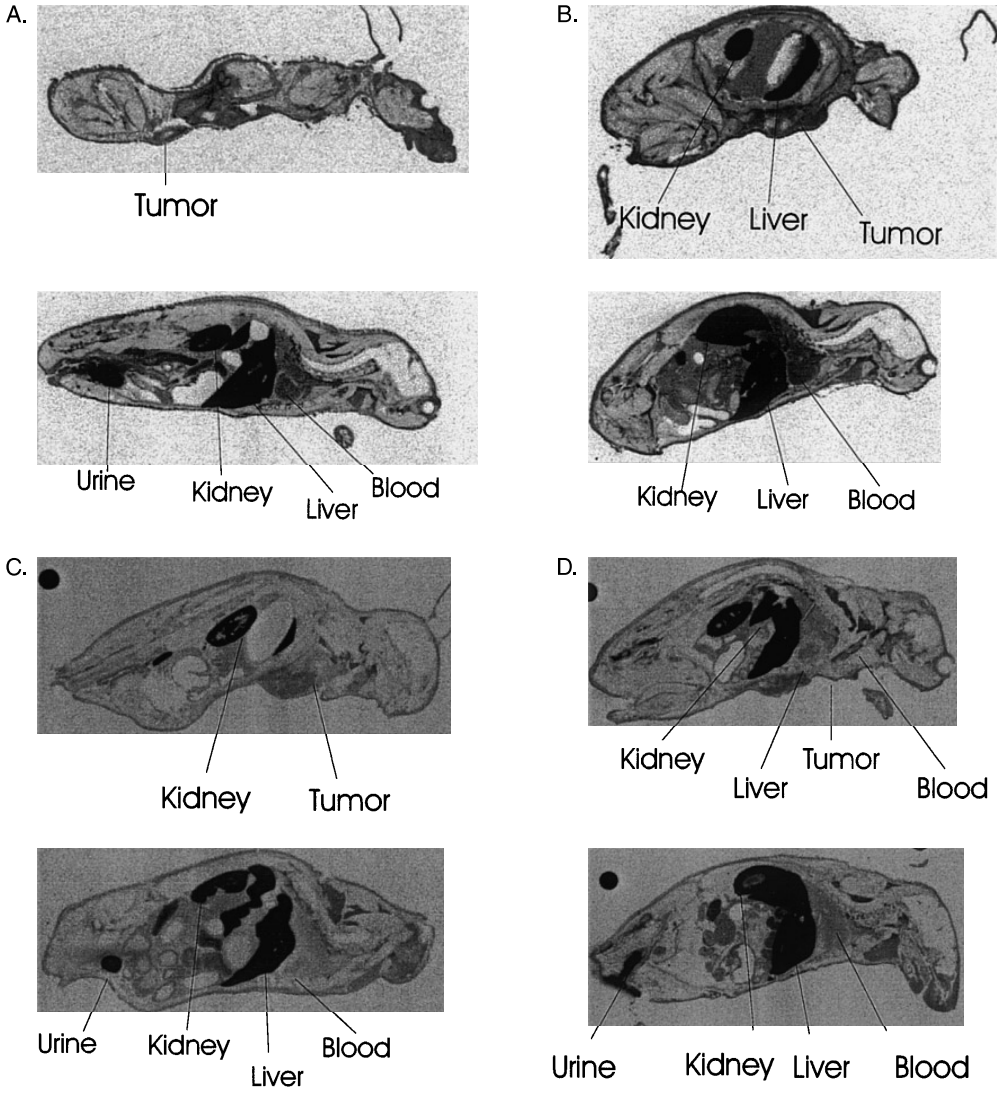

Fig. 3A–D Whole-body autoradiograms 5 min after i.v. administration of [^{14}C]LY309887 and [^{14}C] lometrexol in C3H mammary tumor-bearing mice. Tissue distribution of total radiocarbon, represented by the darkened areas, associated with [^{14}C]LY309887 in mice on LFD (**A**) and SD (**B**) and with [^{14}C]lometrexol in mice on LFD (**C**) and SD (**D**)

Standard curves associated with individual scans were fitted with a least squares regression line from which tissue concentrations of radiocarbon were interpolated. The reported lower limits of detection were based on the mean standard curve concentrations.

Determination of polyglutamate distribution by HPLC

All data generated from the harvesting and extraction of murine liver are averages of two separate experiments. At each time-point, one mouse per experimental group was euthanized by CO_2 asphyxiation. Livers were perfused through the atrium with 5 ml ice-cold phosphate-buffered saline, removed, weighed and extracted by homogenization in an equal volume of ice-cold 20% trichloroacetic acid (Tekmar Tissuemizer, Cincinnati, Ohio). Homogenates were centrifuged at 60 000 rpm (195 000 *g*) for 30 min at 4 °C in a Beckman TL-100 ultracentrifuge. Supernatants were neutralized by dropwise addition of 1 *N* or 5 *N* NaOH, final volumes were measured and the samples were stored at −20 °C. Supernatants were clarified by centrifugation (14 000 *g*, 10 min) prior to chromatography by HPLC (500 µl) using a modification of the reversed-phase method described by Montero and Llorente [13]. Our protocol utilized a 4.6 mm × 25 cm Beckman Ultrasphere IP 5 µm column, 1.5 ml/min flow rate, and the following gradient elution (v/v): (1) 100% *A* (0.1 *M* ammonium acetate pH 5.5 + 1% acetonitrile) for 5 min, (2) linear gradient to 9% *B* (acetonitrile) over 20 min, (3) 5 min at 9% *B*, (4) linear gradient to 100% *B* over 5 min, (5) linear gradient to 100% *A* over 5 min, (6) 2 min at 100% *A*. UV absorbance data were collected at 278 nm, and the radioisotope detector (Beckman System Gold) ran at a flow rate of 4.5 ml/min using Beckman Ready Flow III cocktail.

The distribution of parent compound and polyglutamates was calculated from the amount of radiocarbon incorporated into the peaks in counts per minute. Mono- and polyglutamate elution times for this protocol were previously determined by chromatography of synthesized standards and in vitro polyglutamation reactions. Retention times for parent compound LY309887 (defined as the monoglutamate), di-, tri-, tetra-, penta-, and hexaglutamate were: 26.1, 22.6, 20.4, 18.8, 17.6, and 16.6 min, respectively. Retention times for lometrexol, di-, tri-, tetra-, penta-, hexa-, hepta-, and octaglutamate were: 27.3, 24.1, 21.6, 20.0, 18.8, 18.2, 17.7, and 17.3 min, respectively. The sensitivities for detection of LY309887 and lometrexol were 13 and 88 pmol, respectively.

Results

Quantitative whole-body autoradiographic evaluation of [^{14}C]LY309887 and [^{14}C]lometrexol

Radiocarbon concentrations were quantitated in blood, kidney, liver, and tumor with a lower limits of detection

for [^{14}C]LY309887 of 380 pmol/g and for [^{14}C]lometrexol of 2300 pmol/g. The time-dependent distribution of radiolabeled LY309887 and lometrexol in four tissues from SD and LFD mice assessed by autoradiography is shown in Fig. 2. Representative phosphor imaging-generated autoradiograms showing the tissue distribution of total radiocarbon associated with [^{14}C]LY309887 and [^{14}C]lometrexol at 5 min and 168 h postdose are presented in Figs. 3 and 4.

At 5 min postdose, total radiocarbon was widely distributed into most major tissues including kidney, liver, and mammary tumor in all mice (Fig. 3). Radiocarbon in blood was detected in all mice except the [^{14}C]lometrexol/SD mouse at 5 min postdose, and by 6 h postdose radiocarbon in blood was quantitatively detectable only in the [^{14}C]LY309887/LFD mouse which had blood concentrations of 1514 pmol/g. At 24 h postdose, blood concentrations of radiocarbon associated with [^{14}C]LY309887 had declined to below the detectable limit of 380 pmol/g.

Kidney had high concentrations of radiocarbon at 5 min postdose for all mice ranging from approximately 12 909 pmol/g in the [^{14}C]lometrexol/LFD mouse to 7720 pmol/g in the [^{14}C]LY309887/LFD mouse. Kidney radiocarbon concentrations were consistently higher following [^{14}C]lometrexol administration in LFD mice than following [^{14}C]LY309887 administration. At 24 h postdose, the LFD mice had approximately four-fold greater concentrations of [^{14}C]lometrexol than [^{14}C]LY309887 (Fig. 2). Kidney concentrations declined most rapidly in mice on SD, while in mice on LFD, drug concentrations were still detectable at 168 h postdose with concentrations of 2069 and 2530 pmol/g following [^{14}C]LY309887 and [^{14}C]lometrexol administration, respectively (Fig. 4).

High and sustained liver concentrations of radiocarbon associated with both compounds were observed in the LFD mice at all time-points. Liver concentrations of radiocarbon associated with [^{14}C]lometrexol averaged two-fold higher than radiocarbon associated with [^{14}C]LY309887 at all time-points after 5 min (Figs. 2 and 4). In SD mice, [^{14}C]lometrexol concentrations exceeded [^{14}C]LY309887 concentrations between 5 min and 48 h, ranging from 2-fold at 5 min to 5.5-fold at 48 h (3823 and 690 pmol/g, respectively). At 96 and 120 h in SD mice, only radiocarbon associated with [^{14}C]LY309887 was detectable because the amount of lometrexol was below its threshold for detection. No radiocarbon associated with either compound was detectable at 168 h. However, radioactivity could still be detected using liquid scintillation spectrometry at all times and under all dietary conditions, as reported below.

Initial tumor concentrations of radiocarbon associated with [^{14}C]lometrexol (7978 pmol/g for LFD and 7701 pmol/g for SD) were approximately six-fold greater than radiocarbon associated with [^{14}C]LY309887 (1067 pmol/g for LFD and 1379 pmol/g for SD). However, only tumors in LFD mice following [^{14}C]LY309887 administration retained quantifiable levels of radiocarbon at the later time-points. Low concentrations of 467 pmol/g were still detectable at 120 h postdose (Fig. 2).

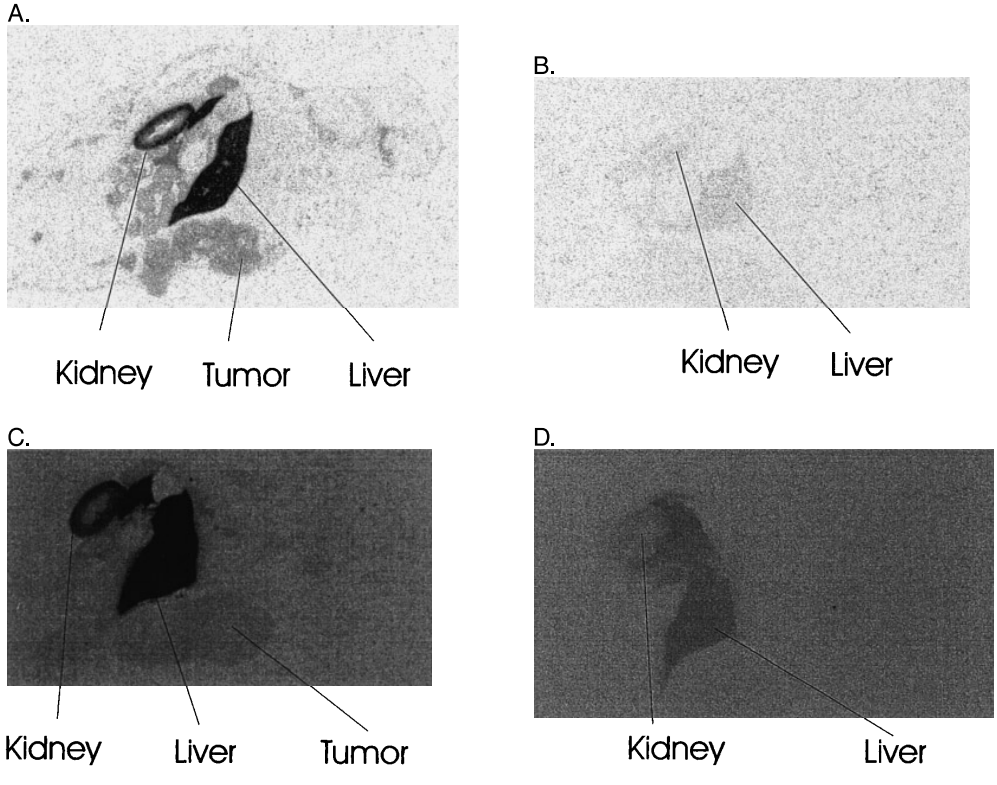

Fig. 4A–D Whole-body autoradiograms 168 h after i.v. administration of [^{14}C]LY309887 and [^{14}C]lometrexol in C3H mammary tumor-bearing mice. Tissue distribution of total radiocarbon, represented by the darkened areas, associated with [^{14}C]LY309887 in mice on LFD (**A**) and SD (**B**) and with [^{14}C]lometrexol in mice on LFD (**C**) and SD (**D**)

Distribution of polyglutamates in murine liver

Using reversed-phase HPLC, polyglutamation of LY309887 and lometrexol in livers from mice maintained on SD or LFD was determined (Fig. 5). In SD livers, hexaglutamates of both compounds were first detected 24 h after dosing and were the longest species seen through 168 h. After 24 h, pentaglutamates of both compounds were the major species. Thus, at all times livers from SD mice accumulated more lometrexol than LY309887 (Fig. 2), but the profiles of polyglutamates obtained for each compound were similar (Fig. 5A).

In LFD livers, hexaglutamates of both compounds were first detected at 6 h (Fig. 5B). Pentaglutamates of LY309887 predominated after 6 h, and hexaglutamates were the longest species detected. Similarly, penta- and hexaglutamates of lometrexol predominated after 24 h. However, in livers from mice on LFD, approximately 14% of the lometrexol was further polyglutamated to the hepta- and octaglutamates at 168 h.

Discussion

LY309887 is a second generation GARFT inhibitor currently in phase 1 clinical trials for the treatment of solid tumors. The unexpected delayed toxicity seen with lometrexol in phase 1 studies and the clinical observation that oral folate supplementation prevents these toxicities led us to measure and compare the time-dependent effect of changes in dietary folate on accumulation of these two compounds in murine liver, tumor and other organs. Administration of single equimolar i.v. bolus doses of each GARFT inhibitor allowed a direct pharmacokinetic comparison of tissue accumulation of the two compounds. Preliminary experiments had demonstrated that at this low nonefficacious dose all mice, including LFD mice, would survive longer than the 7 days required to complete the studies. Whole-body autoradiography revealed that the highest concentrations of compound were deposited in livers of mice from the LFD/lometrexol group followed (in descending order) by the livers from the mice in the LFD/LY309887, SD/lometrexol, and SD/LY309887 groups (Fig. 2). A previous study in which a 30 mg/kg i.v. bolus dose of

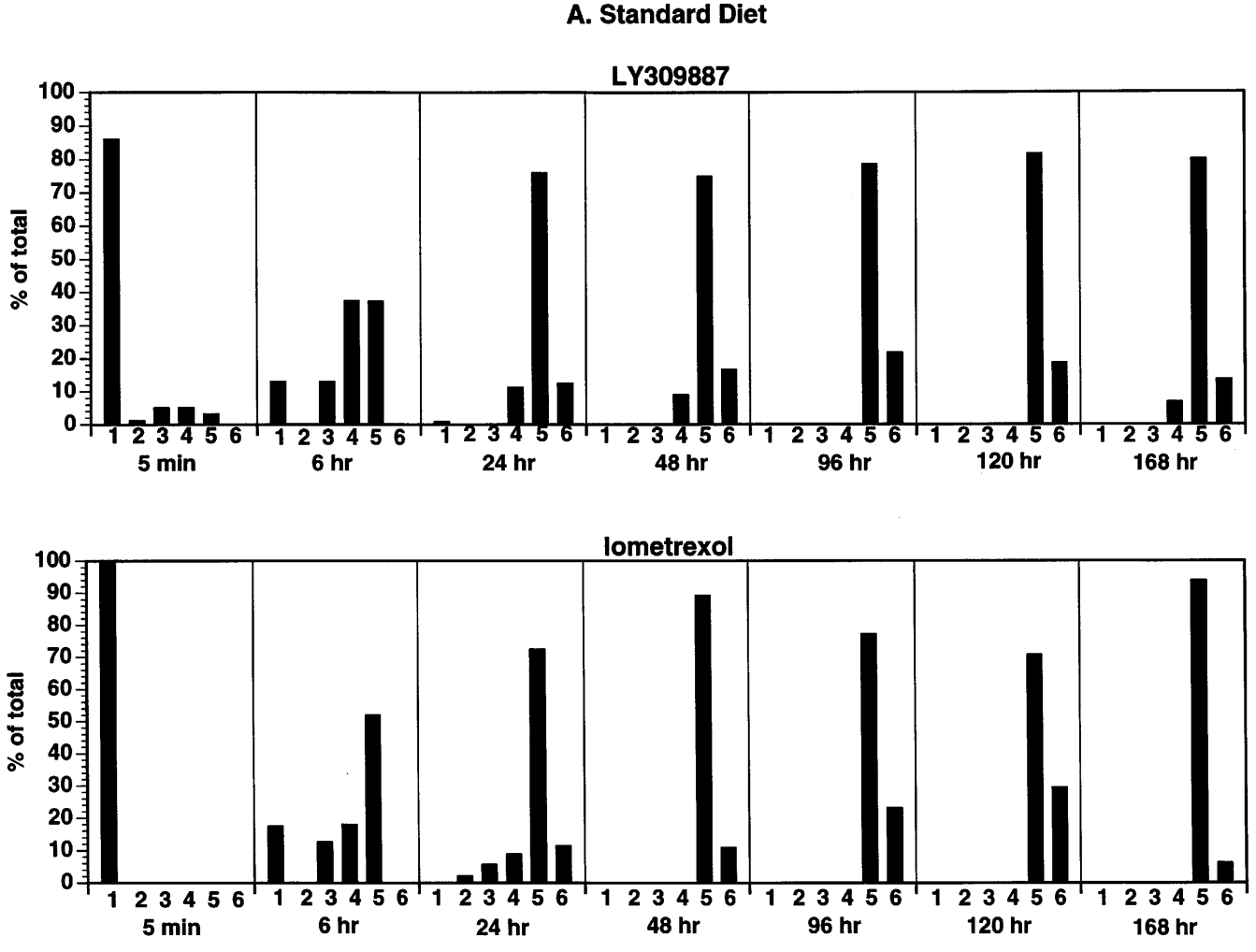

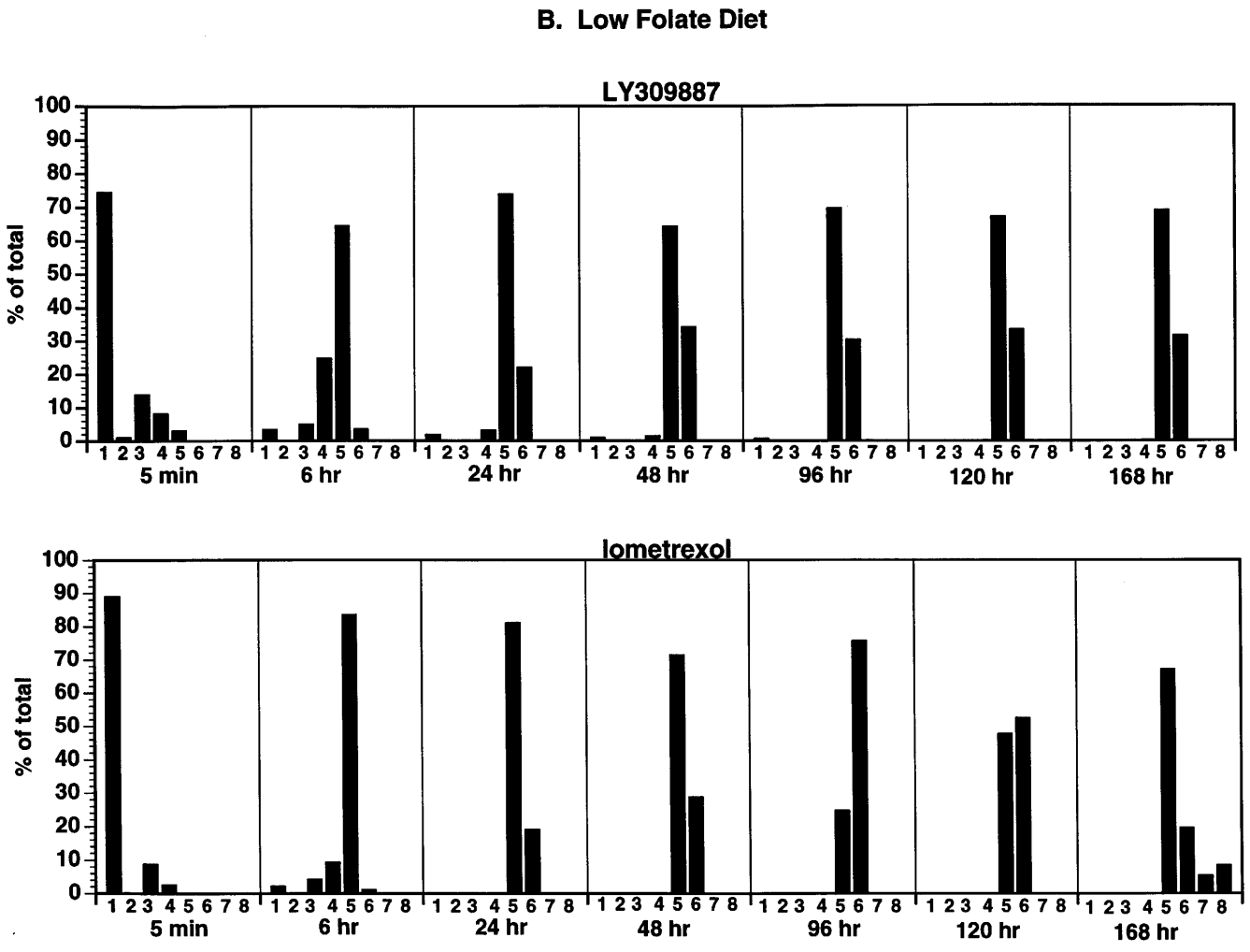

Fig. 5A,B Polyglutamate distribution in murine liver. The distributions of parent compound and polyglutamate forms for [^{14}C]LY309887 and [^{14}C]lometrexol in livers of mice on (**A**) SD and (**B**) LFD over time are shown. The numbers 1–6 indicate the number of glutamate residues (one glutamate residue = parent compound). *Bars* represent the percentage of total peak area in counts per minute found for each (poly)glutamate species at each time-point, and the values indicated are the average of two independent determinations

lometrexol was given to mice on SD or LFD also resulted in greater deposition in livers from mice on LFD [15].

Although the factors responsible for the greater accumulation of lometrexol than of LY309887 in murine liver have not been definitively determined, several known processes may contribute. Lometrexol and LY309887 are thought to utilize the reduced folate carrier for uptake at high, micromolar concentrations, and folate receptors at low serum concentrations [25]. In addition, LY309887 has greater selectivity for the α (nonliver) isoform of murine and human folate receptors than lometrexol [6, 12]. In clinical studies, both compounds have demonstrated long γ-phase half-lives with low (1–50 *n*M) serum concentrations (unpublished observation; [24]). At these levels, selectivity for one folate receptor isoform may have clinical significance and could influence uptake through the hepatic folate receptor β, enterohepatic recirculation and the sustained plasma concentrations of these compounds.

Another factor which may influence liver retention is polyglutamation by FPGS [11]. As a substrate for mammalian FPGS, LY309887 has a 1.4-fold lower first-order rate constant (V_{max}/K_m) for conversion to diglutamate than lometrexol [9]. Consistent with this kinetic property, the results of this study showed that LY309887 was less extensively polyglutamated than lometrexol in LFD murine liver. Alternatively, γ-glutamyl hydrolase [17], the lysosomal enzyme which cleaves folate polyglutamates, may preferentially hydrolyze LY309887 polyglutamates contributing to the less extensive polyglutamation of this compound in livers of LFD mice. Using the same 2-week LFD paradigm that we employed, Schmitz et al. [19] have demonstrated that folate pools from mice on LFD are reduced in plasma, liver, intestine, and tumors. The concentration of folate has been shown to regulate polyglutamation of natural folates and antifolates in vitro, through modulation of purified FPGS activity, as well as intracellularly [5]. For

both GARFT inhibitors, lower concentrations of competing natural folate substrates in LFD mice resulted in higher percentages of longer chain polyglutamates at earlier times than in mice on SD. In addition, mice on LFD have 50% higher liver FPGS activity [7], which may also contribute to the earlier formation of longer polyglutamates in liver from mice on LFD than in those on SD. Collectively, transport and polyglutamation of these GARFT inhibitors by the liver and the effect of dietary folate on liver retention may influence the duration of the γ-phase half-life of these compounds and their potential for delayed toxicity.

The higher specific activity of [^{14}C]LY309887 and its corresponding lower limit of detection resulted in greater sensitivity at longer time-points in tissues containing low concentrations of [^{14}C]LY309887. In blood, [^{14}C]lometrexol (limit of detection 2300 pmol/g) was not detectable after 6 h, whereas a low concentration of [^{14}C]LY309887 (limit of detection 380 pmol/g) was detectable (Fig. 2). In kidney, as in liver, [^{14}C]lometrexol accumulated to higher concentrations than [^{14}C]LY309887. The highest sustained concentrations of both compounds were in liver followed (in decreasing concentration) by kidney, tumor and blood. In all these tissues clearance was more rapid in SD mice than in LFD mice. The increased rate of drug clearance in folate-replete animals is consistent with the use of folic acid and leucovorin to rescue patients experiencing toxicity [20].

The highest sustained drug concentrations in C3H tumors were found in the LFD/LY309887 group. Higher drug concentrations in tumors from LFD mice may be attributable to lower concentrations of competing natural folates, and elevations in FPGS activity which increases in many tumors in mice on LFD [7].

In summary, LY309887 has a unique profile consisting of greater potency to inhibit GARFT, greater antitumor potency, a lower efficiency as a substrate for mammalian FPGS, and lower affinity for liver folate receptor than lometrexol. These characteristics are consistent with its reduced accumulation in liver, and suggest that LY309887 may produce clinical responses at lower doses than lometrexol and have less potential to produce delayed cumulative toxicity. Despite this improved pharmacological profile, nutritional folate supplementation to manage folate status appears to be necessary for drugs of this class.

Acknowledgements We gratefully acknowledge the expert technical assistance of Jennifer L. Herman, Tracy D. Self, and William Joe Wheeler (Lilly Research Laboratories, Indianapolis, Ind.).

References

1. Alati T, Worzalla JF, Shih C, Bewley JR, Lewis S, Moran RG, Grindey GB (1996) Augmentation of the therapeutic activity of lometrexol [(6-R)5,10-dideazatetrahydrofolate] by oral folic acid. Cancer Res 56: 2331–2335
2. Baldwin SW, Tse A, Gossett LS, Taylor EC, Rosowsky A, Shih C, Moran RG (1991) Structural features of 5,10-dideaza-5,6,7,8-tetrahydrofolate that determine inhibition of mammalian glycinamide ribonucleotide formyltransferase. Biochemistry 30: 1997–2006
3. Brigle KE, Spinella MJ, Westin EH, Goldman ID (1994) Increased expression and characterization of two distinct folate binding proteins in murine erythroleukemia cells. Biochem Pharmacol 47: 337–344
4. Chay SH, Pohland RC (1994) Comparison of quantitative whole-body autoradiographic and tissue dissection techniques in the evaluation of the tissue distribution of [^{14}C]daptomycin in rats. J Pharm Sci 83: 1294–1299
5. Cook JD, Cichowicz DJ, George S, Lawler A, Shane B (1987) Mammalian folylpoly-γ-glutamate synthetase. 4. In vitro and in vivo metabolism of folates and analogues and regulation of folate homeostasis. Biochemistry 26: 530–539
6. Gates SB, Mendelsohn LG, Shackelford KA, Habeck LL, Kursar JD, Gossett LS, Worzalla JF, Shih C, Grindey GB (1996) Characterization of folate receptor from normal and neoplastic murine tissue: influence of dietary folate on folate receptor expression. Clin Cancer Res 2: 1135–1141
7. Gates SB, Schultz RM, Self TD, Grindey GB, Mendelsohn LG (1996) Folylpolyglutamate synthetase activity in normal and neoplastic murine tissues and human tumor xenografts. Biochem Pharmacol 52:1477–1479
8. Habeck LL, Leitner TA, Shackelford KA, Gossett LS, Schultz RM, Andis SL, Shih C, Grindey GB, Mendelsohn LG (1994) A novel class of monoglutamated antifolates exhibits tight-binding inhibition of human glycinamide ribonucleotide formyltransferase and potent activity against solid tumors. Cancer Res 54: 1021–1026
9. Habeck LL, Mendelsohn LG, Shih C, Taylor EC, Colman PD, Gossett LS, Leitner TA, Schultz RM, Andis SL, Moran RG (1995) Substrate specificity of mammalian folylpolyglutamate synthetase for 5,10-dideazatetrahydrofolate analogs. Mol Pharmacol 48: 326–333
10. Johnston RF, Pickett SC, Barker DL (1990) Autoradiography using storage phosphor technology. Electrophoresis 11: 355–360
11. McGuire JJ, Bertino JR (1981) Enzymatic synthesis and function of folylpolyglutamates. Mol Cell Biochem 39: 19–48
12. Mendelsohn LG, Shih C, Schultz RM, Worzalla JF (1996) Biochemistry and pharmacology of glycinamide ribonucleotide formyltransferase inhibitors: LY309887 and lometrexol. Invest New Drugs 14: 287–294
13. Montero C, Llorente P (1993) Single step LC method for determination of folylpolyglutamate synthetase activity and separation of polyglutamates. Chromatographia 37: 73–78
14. Moran RG, Baldwin SW, Taylor EC, Shih C (1989) The 6S- and 6R-diastereomers of 5,10-dideaza-5,6,7,8-tetrahydrofolate are equiactive inhibitors of *de novo* purine synthesis. J Biol Chem 264: 21047–21051
15. Pohland RC, Alati T, Lantz RJ, Grindey GB (1994) Whole-body autoradiographic disposition and plasma pharmacokinetics of 5,10-dideazatetrahydrofolic acid in mice fed folic-acid deficient or regular diets. J Pharm Sci 83: 1396–1399
16. Ray MS, Muggia FM, Leichman GC, Nelson RL, Dyke RW, Moran RG (1993) Phase I study of 6(R)-5,10-dideazatetrahydrofolate: a folate antimetabolite inhibitory to *de novo* purine synthesis. J Natl Cancer Inst 85: 1154–1159
17. Rhee MS, Wang Y, Nair MG, Galivan J (1993) Acquisition of resistance to antifolates caused by enhanced γ-glutamyl hydrolase activity. Cancer Res 53: 2227–2230
18. Ross JF, Chaudhuri PK, Ratnam M (1994) Differential regulation of folate receptor isoforms in normal and malignant tissues in vivo and in established cell lines. Cancer 73: 2432–2443
19. Schmitz JC, Grindey GB, Schultz RM, Priest DG (1994) Impact of dietary folic acid on reduced folates in mouse plasma and tissues: relationship to dideazatetrahydrofolate sensitivity. Biochem Pharmacol 48: 319–325
20. Sessa C, de Jong J, D'Incalci M, Hatty S, Pagani O, Cavalli F (1996) Phase 1 study of the antipurine antifolate lometrexol

(DDATHF) with folinic acid rescue. Clin Cancer Res 2: 1123–1127
21. Ullberg S (1977) The technique of whole-body autoradiography: Cryosectioning of large specimens. (Science tools) The LKB Instrument Journal, Special Issue, pp 2–29
22. Wang X, Shen F, Freisheim JH, Gentry LE, Ratnam M (1992) Differential stereospecificities and affinities of folate receptor isoforms for folate compounds and antifolates. Biochem Pharmacol 44: 1898–1901
23. Ward WHJ, Kimbell R, Jackman AL (1992) Kinetic characteristics of ICI D1694: a quinazoline antifolate which inhibits thymidylate synthase. Biochem Pharmacol 43: 2029–2031
24. Wedge SR, Laohavinij S, Taylor GA, Boddy A, Calvert HA, Newell DR (1995) Clinical pharmacokinetics of the antipurine antifolate (6R)-5,10-dideaza-5,6,7-tetrahydrofolic acid (lometrexol) administered with an oral folic acid supplement. Clin Cancer Res 1: 1479–1486
25. Westerhof GR, Schornagel JH, Kathmann I, Jackman AL, Rosowsky A, Forsch RA, Hynes JB, Boyle FT, Peters GJ, Pinedo HM, Jansen G (1995) Carrier- and receptor-mediated transport of folate antagonists targeting folate-dependent enzymes: correlates of molecular-structure and biological activity. Mol Pharmacol 48: 459–471
26. Worzalla JF, Bewley JR, Grindey GB (1990) Automated measurement of transplantable solid tumors using digital electronic calipers interfaced to a microcomputer. Invest New Drugs 8: 241–251
27. Young CW, Currie VE, Muindi JF, Saltz LB, Pisters KMW, Esposito AJ, Dyke RW (1992) Improved clinical tolerance of lometrexol with oral folic acid. Proc Am Assoc Cancer Res 33: 406